

## Controlled synthesis of $\text{ACo}_2\text{O}_4$ (A=Fe, Cu, Zn, Ni) as environmentally friendly electrocatalyst for urea electrolysis

Ping Li<sup>a</sup>, Yanhong Wang<sup>a</sup>, Xiaoqiang Du<sup>a\*</sup> and Xiaoshuang Zhang<sup>b</sup>

<sup>a</sup> School of Chemistry and Chemical Engineering, North University of China, Xueyuan road 3, Taiyuan 030051, People's Republic of China. E-mail: duxq16@nuc.edu.cn

<sup>b</sup> School of Environment and Safety Engineering, North University of China, Xueyuan road 3, Taiyuan 030051, People's Republic of China.

Pretreatment of nickel foam: 4 pieces of nickel foam (3cm×5cm) were ultrasonicated in 3mol/L hydrochloric acid solution and acetone solution for 15min, after which the nickel foam was rinsed several times with ultrapure water and alcohol to remove impurities such as oxides and oil on the surface, dried at 60 °C under vacuum and ready for use.

### DFT computation details:

The DFT calculations were performed using the Cambridge Sequential Total Energy Package (CASTEP) with the plane-wave pseudo-potential method. The geometrical structures of the (111) plane of  $\text{ACo}_2\text{O}_4$  (A=Fe, Cu, Zn, Ni) was optimized by the generalized gradient approximation (GGA) methods. The Revised Perdew-Burke-Ernzerh of (RPBE) functional was used to treat the electron exchange correlation interactions. A Monkhorst Pack grid k-points of 6\*6\*1 of  $\text{ACo}_2\text{O}_4$  (A=Fe, Cu, Zn, Ni), a plane-wave basis set cut-off energy of 500 eV were used for integration of the Brillouin zone. The structures were optimized for energy and force convergence set at 0.05 eV/A and  $2.0 \times 10^{-5}$  eV, respectively.

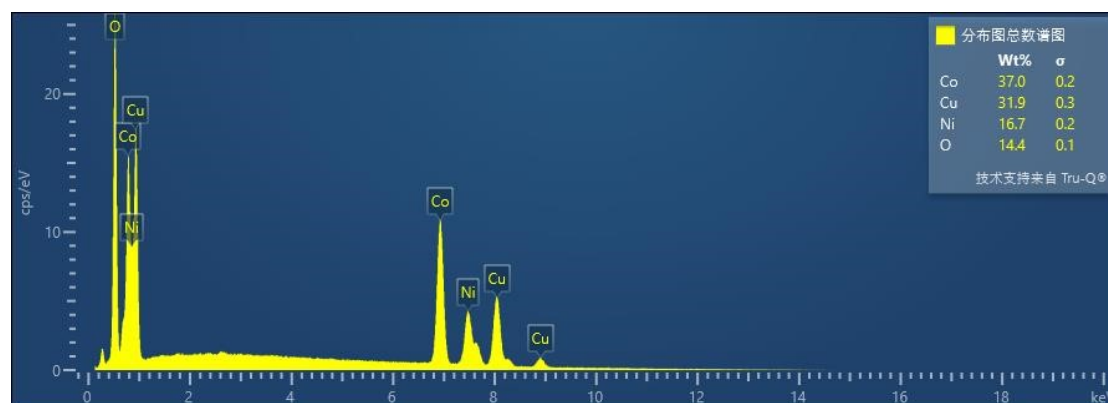


Fig.S1 EDX spectra of the  $\text{CuCo}_2\text{O}_4$  material.

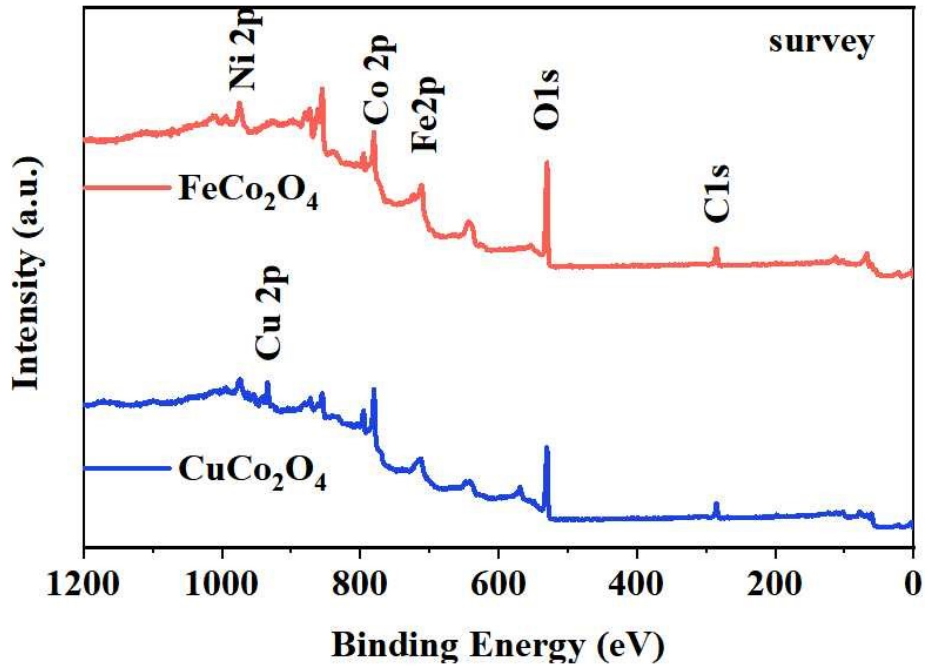


Fig.S2 XPS full spectra of  $\text{FeCo}_2\text{O}_4$  and  $\text{CuCo}_2\text{O}_4$ .

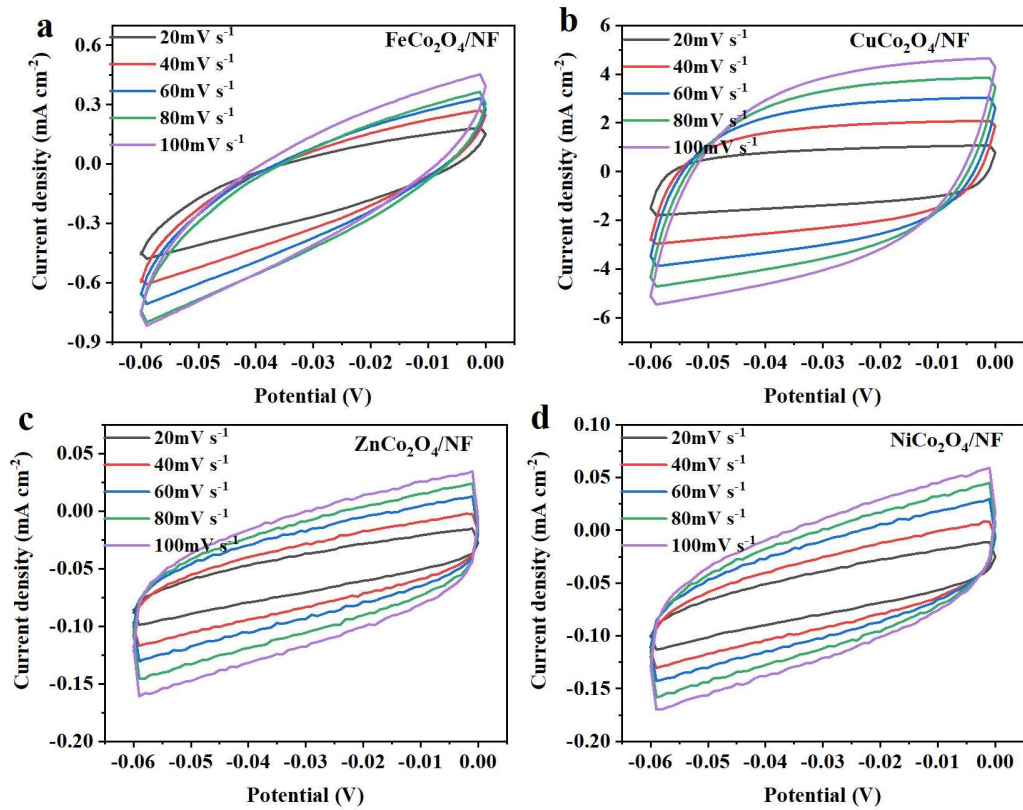


Fig. S3 Cyclic voltammograms (CV) curves of (a) $\text{FeCo}_2\text{O}_4$  ,(b)  $\text{CuCo}_2\text{O}_4$  ,(c)  $\text{ZnCo}_2\text{O}_4$  and  $\text{NiCo}_2\text{O}_4$  for HER.

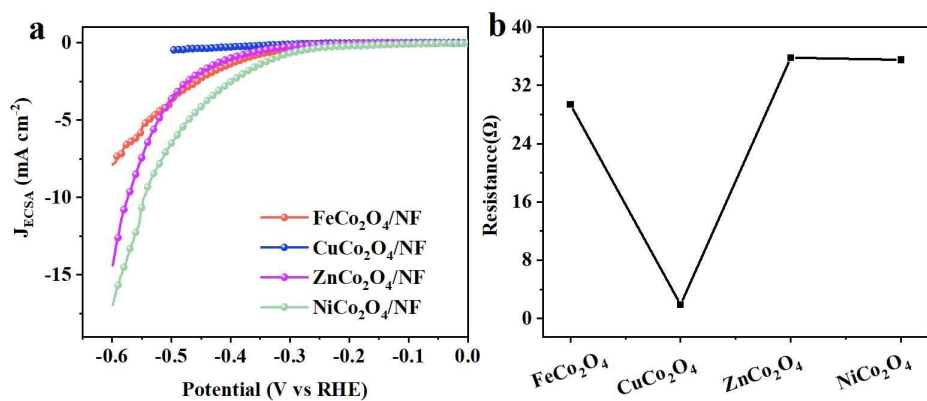


Fig. S4 (a) Normalized ECSA curves and (b) Rct of the ACo<sub>2</sub>O<sub>4</sub>/NF in HER.

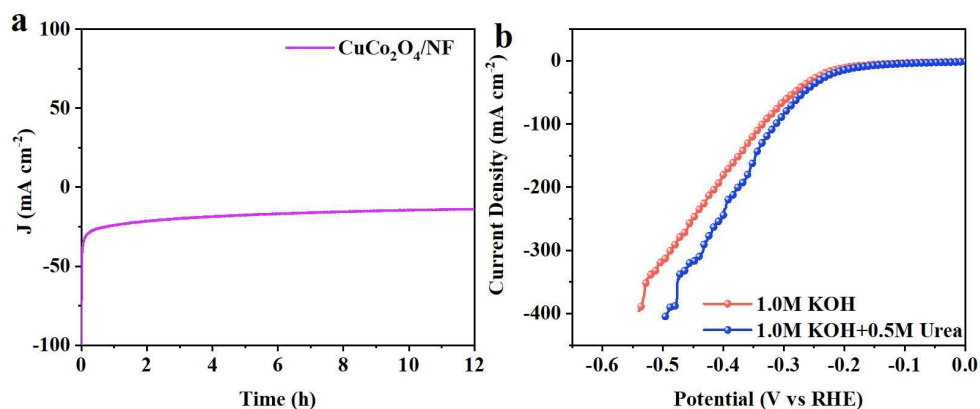


Fig. S5 (a) IT curve for HER, (b) LSV curves of CuCo<sub>2</sub>O<sub>4</sub> in 1.0 M KOH, 1.0 M KOH and 0.5 M urea.

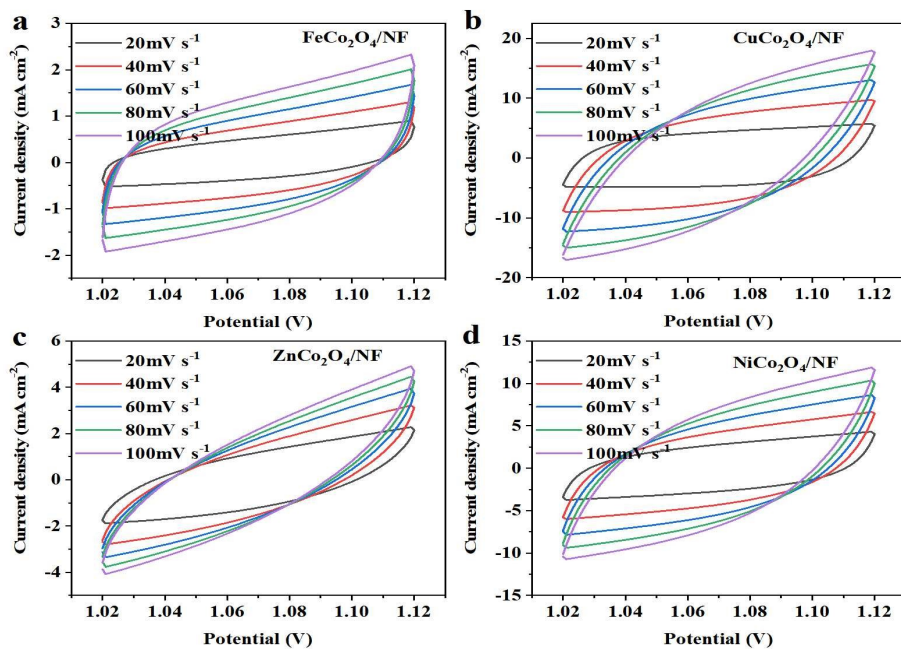


Fig. S6 Cyclic voltammograms (CV) curves of (a) FeCo<sub>2</sub>O<sub>4</sub>, (b) CuCo<sub>2</sub>O<sub>4</sub>, (c) ZnCo<sub>2</sub>O<sub>4</sub> and (d) NiCo<sub>2</sub>O<sub>4</sub>.

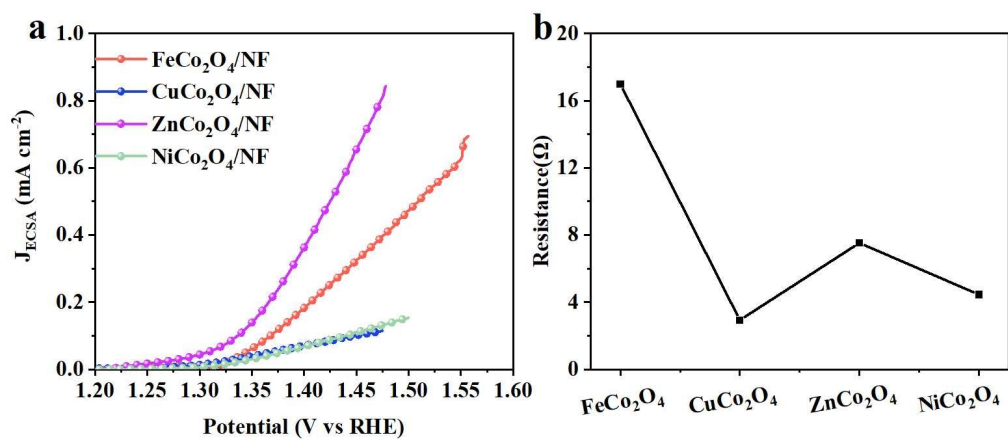


Fig. S7 (a) Normalized ECSA curves and (b)  $R_{ct}$  of the ACo<sub>2</sub>O<sub>4</sub>/NF in UOR.

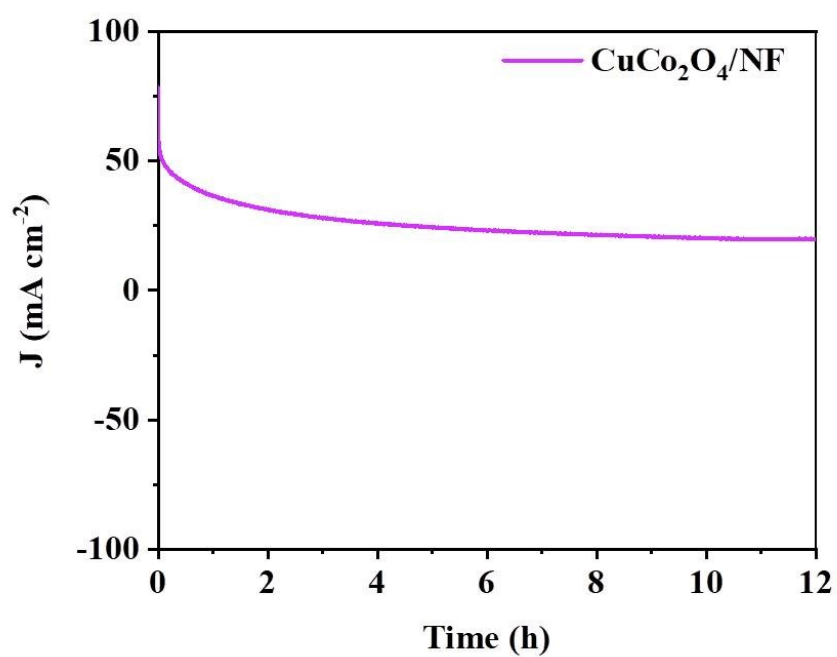
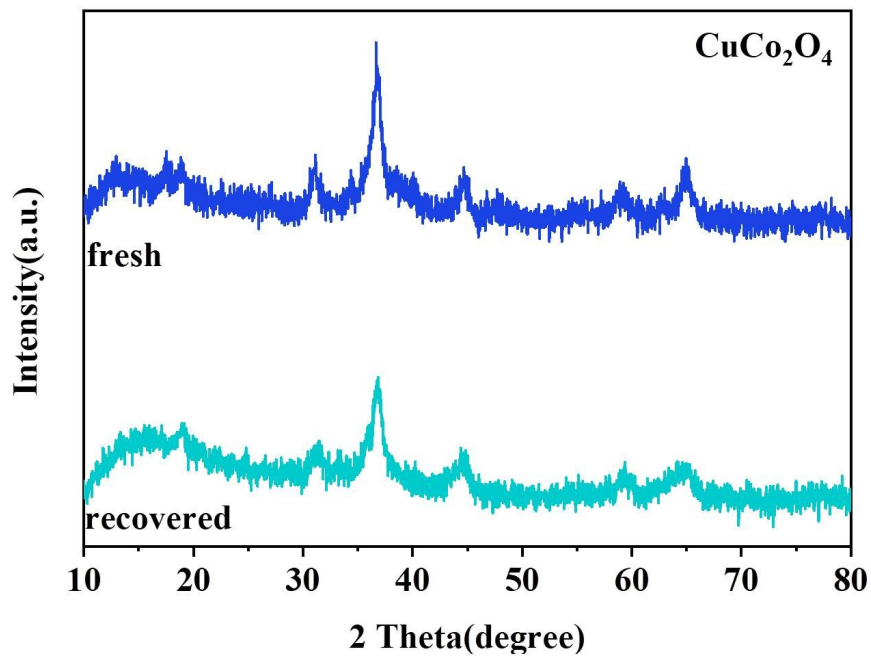
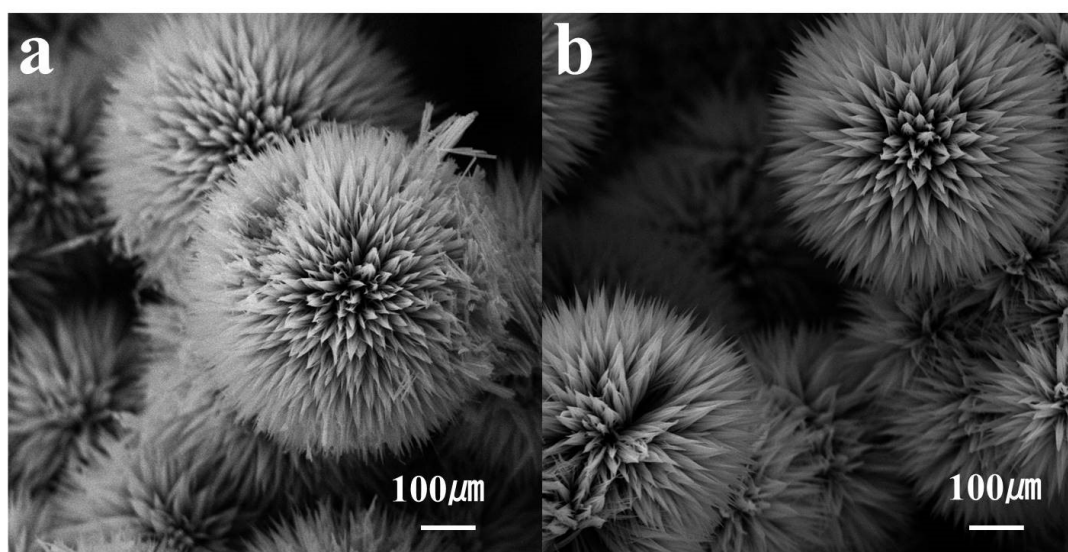


Fig. S8 IT curve of CuCo<sub>2</sub>O<sub>4</sub> for UOR.



**Fig. S9** (a) Fresh and (b) recovered XRD spectra for UOR.



**Fig. S10** (a) Fresh and (b) recovered SEM images for UOR.

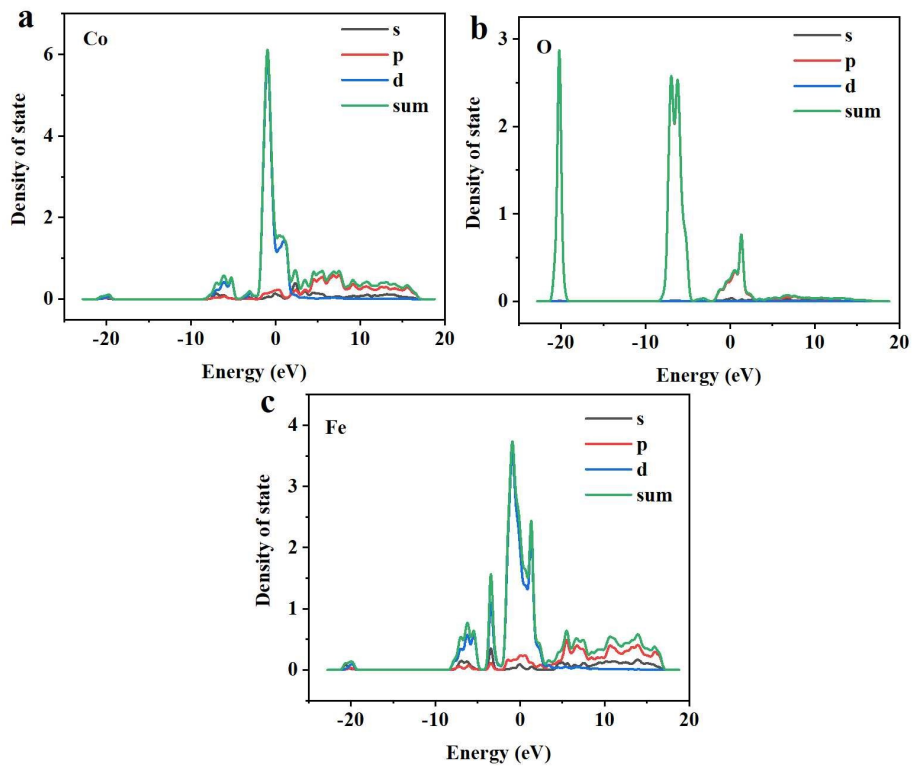


**Fig. S11** Density of states for  $\text{FeCo}_2\text{O}_4$ , (a) Co, (b) O and (c) Fe.

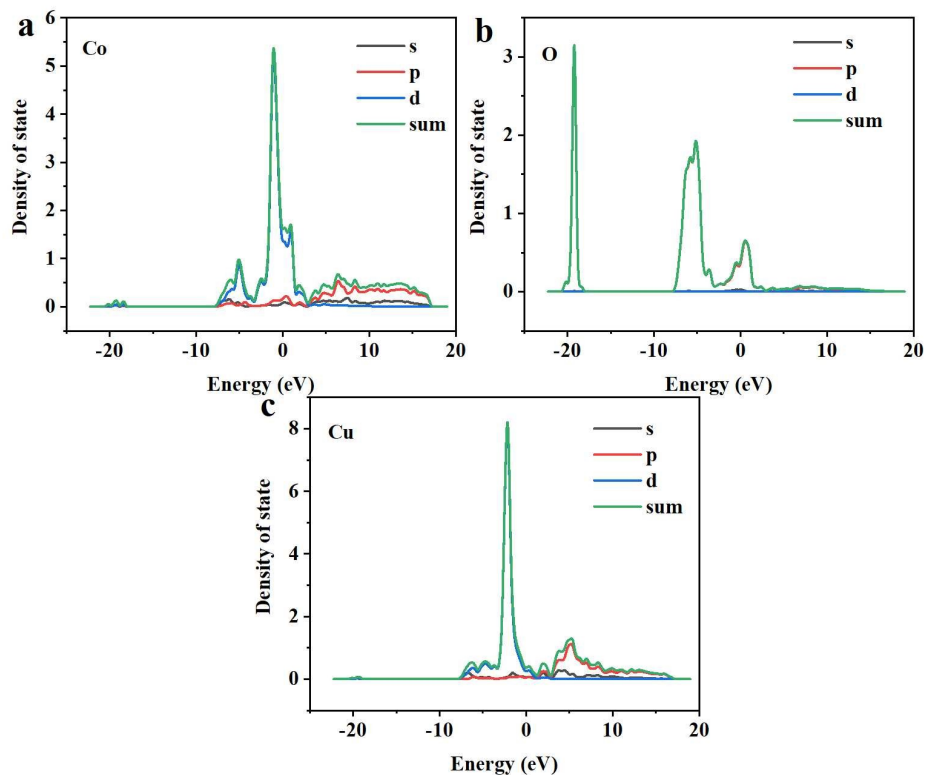


**Fig. S12** Density of states for  $\text{CuCo}_2\text{O}_4$ , (a) Co, (b) O and (c) Cu.

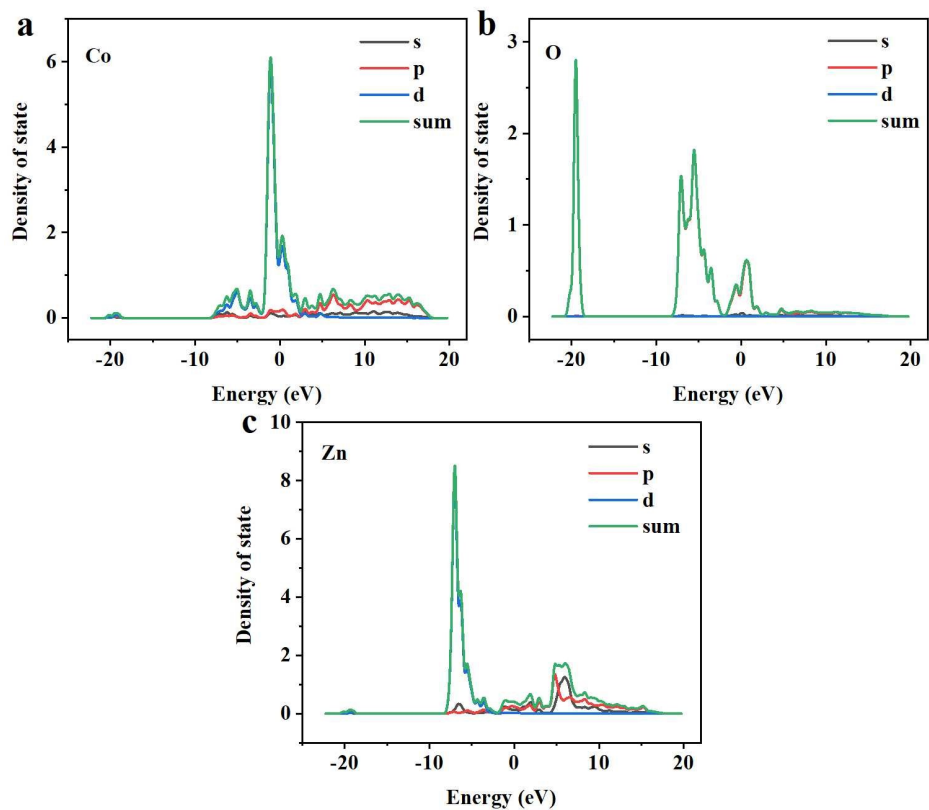


**Fig. S13** Density of states for  $\text{ZnCo}_2\text{O}_4$ , (a) Co, (b) O and (c) Zn.

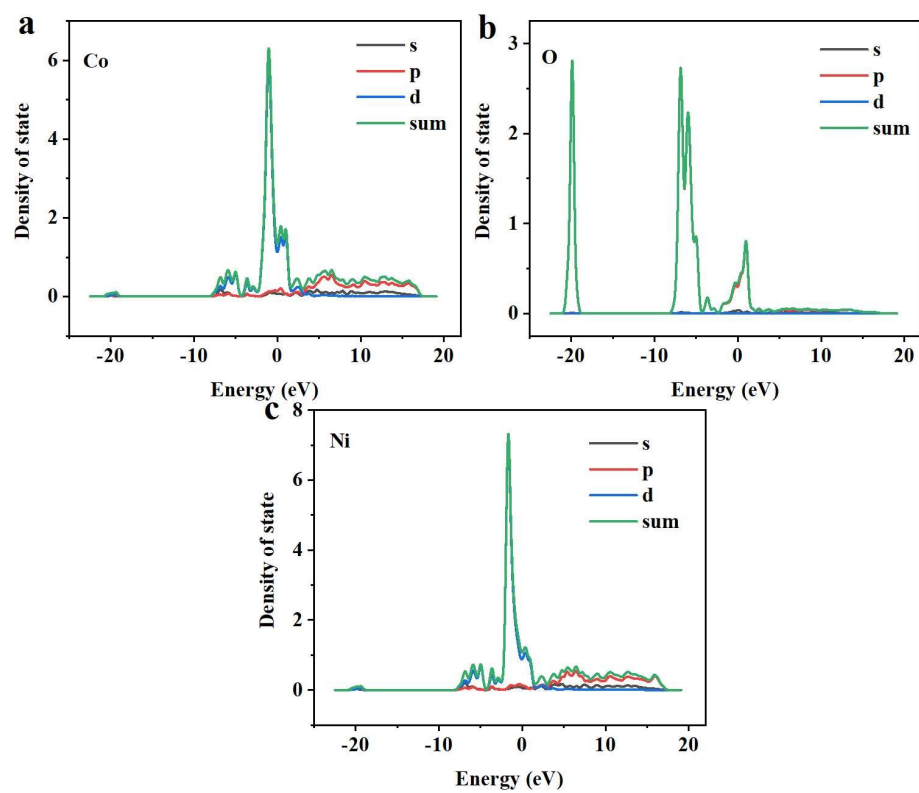


**Fig. S14** Density of states for  $\text{NiCo}_2\text{O}_4$ , (a) Co, (b) O and (c) Ni.

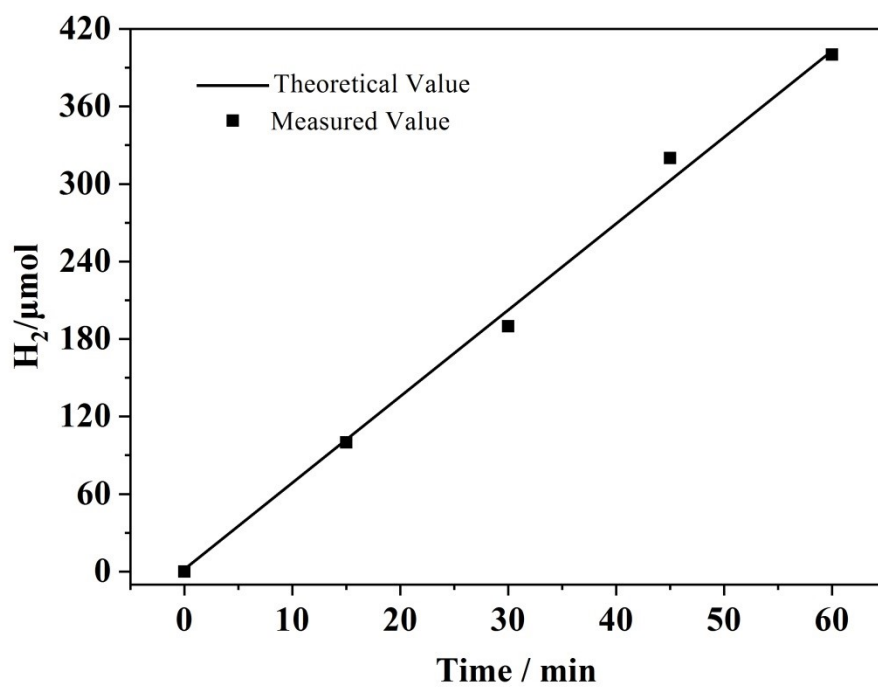


**Fig. S15** Electrocatalytic efficiency of H<sub>2</sub> production over CuCo<sub>2</sub>O<sub>4</sub>/NF.